Supplementary Figure legends

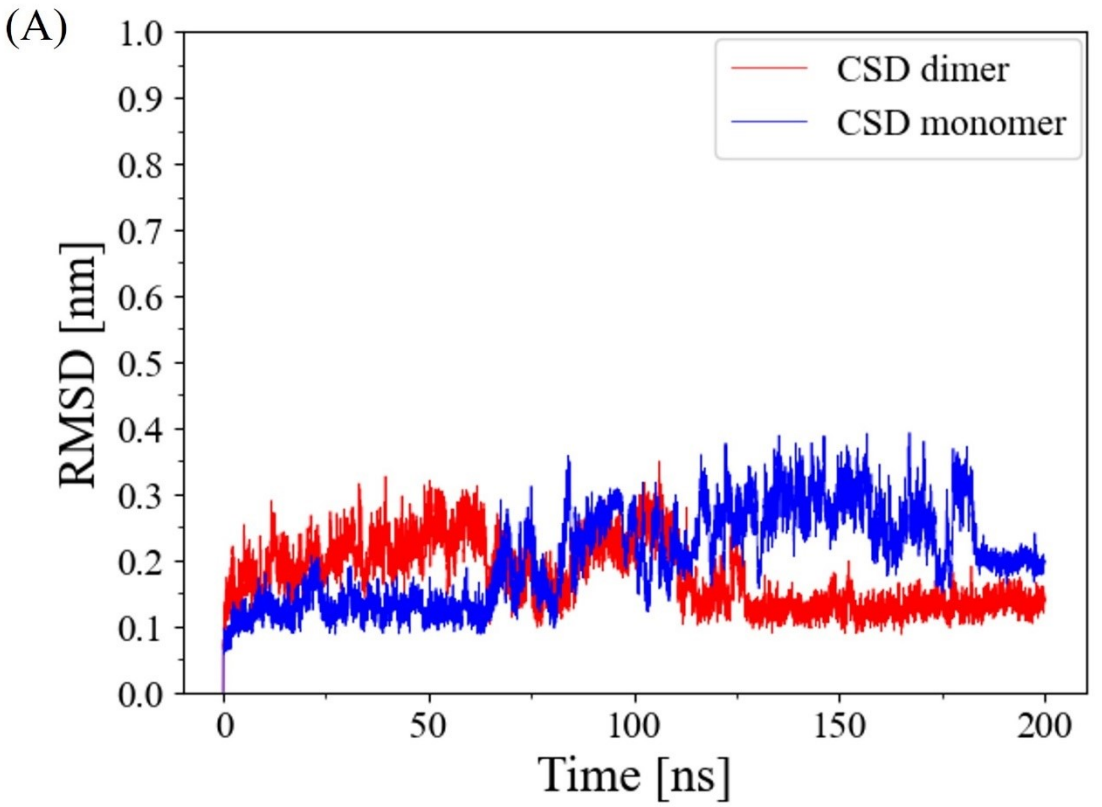

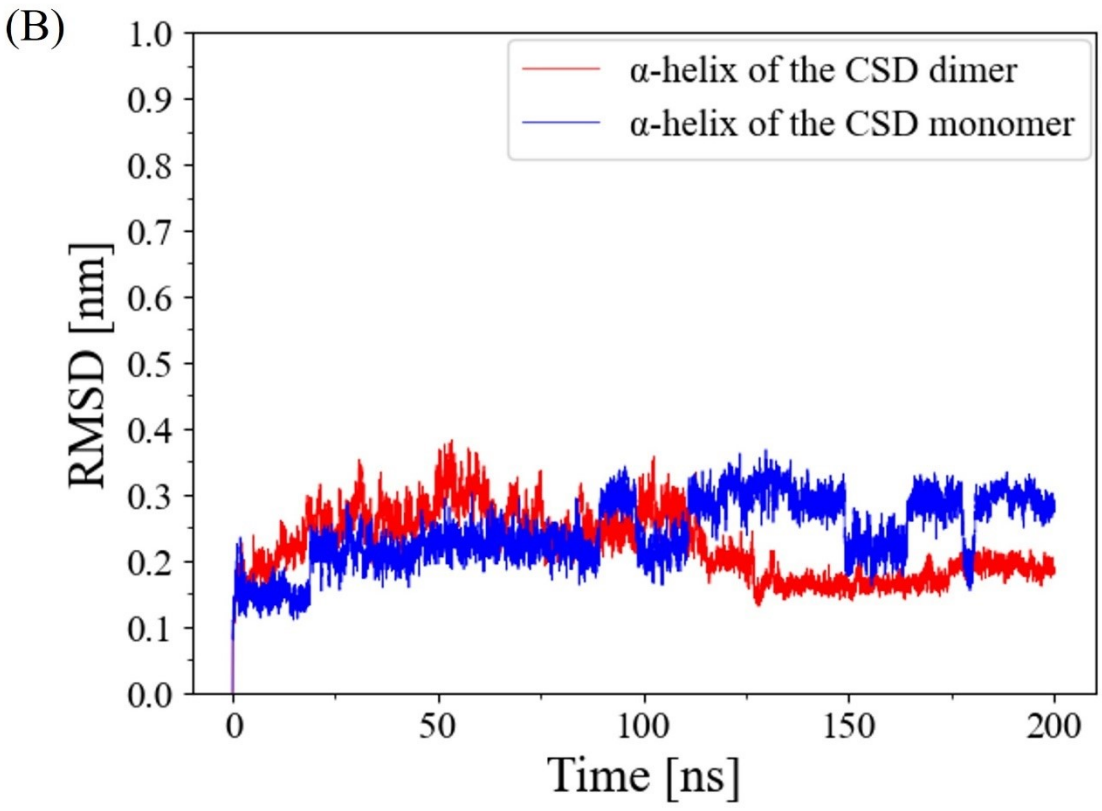

Supplementary Figure S1: Root Mean Square Deviation (RMSD) Analysis CSD Structures Over a 200 ns Relaxation Simulation. Panel A illustrates the RMSD for the entire CSD structure, comparing both dimer and monomer forms. Panel B focuses on the RMSD of individual α-helices within the CSD dimer and monomer. The CSD monomer was derived from the dimer structure (PDB ID: 3I3C) and underwent the same simulation procedures as the CSD-CSD dimer.

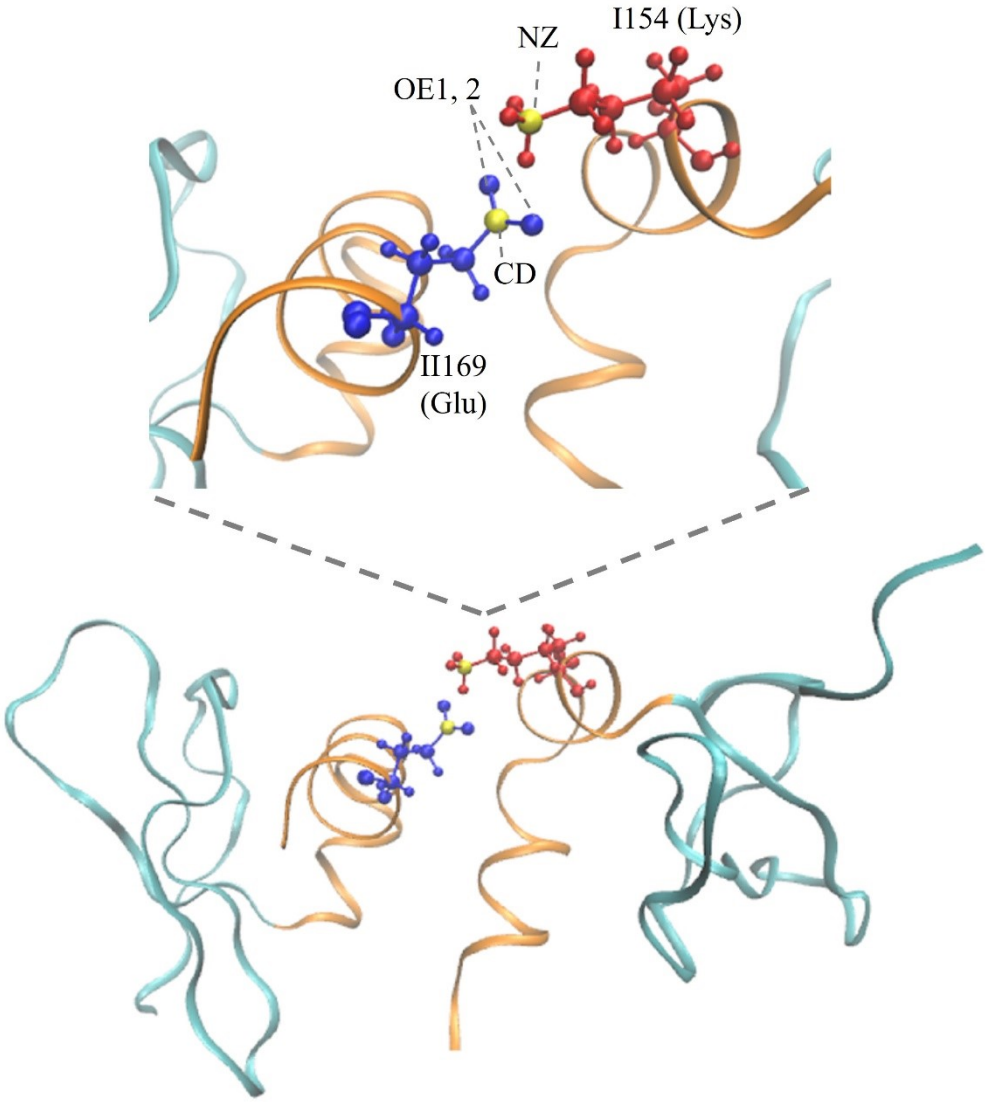

Supplementary Figure S2: Detailed Visualization of the ^{I}Lys154-^{II}Glu169 Salt Bridge in the CSD-CSD Dimer. This figure highlights the residue pairs involved in the salt bridge. Lysine (^{I}Lys154), a positively charged amino acid, is showcased in red, with its key atom, NZ, marked in yellow. Conversely, Glutamic acid (^{II}Glu169), a negatively charged amino acid, is colored in blue, featuring its critical atoms - the delta carbon (CD) and terminal epsilon oxygen atoms (OE1 and OE2) - in yellow. These depictions serve to emphasize the structural details of the salt bridge, with NZ representing the terminal nitrogen atom in lysine's sidechain and CD, OE1, and OE2 indicating the vital components of glutamic acid.

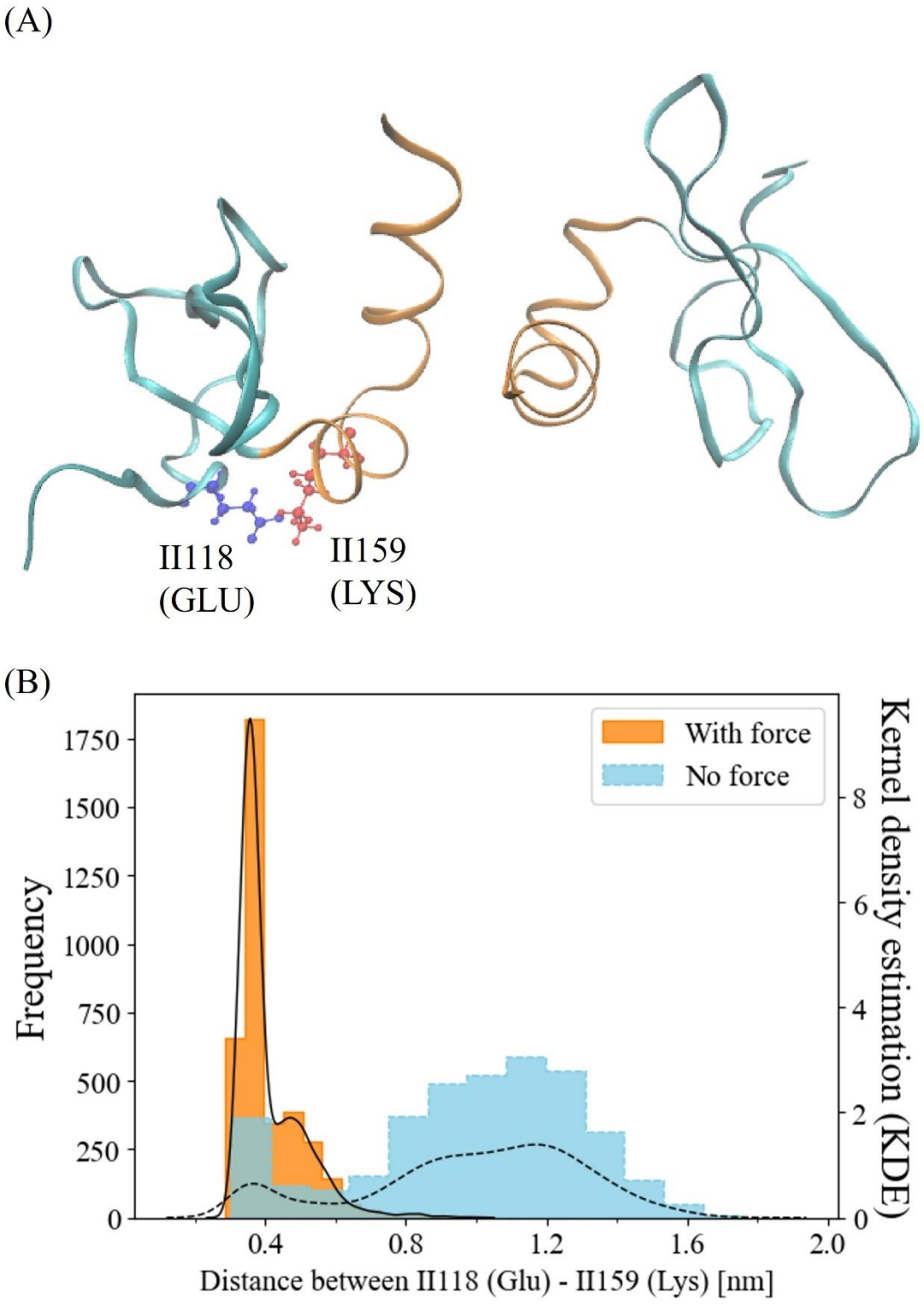

Supplementary Figure S3: Analysis of the ^{II}Glu118-^{II}Lys159 Salt Bridge in the CSD-CSD Dimer. Panel A presents a detailed visualization of the CSD-CSD dimer, focusing on the ^{II}Glu118-

^{II}Lys159 salt bridge. In this depiction, lysine (^{II}Lys159) is shown in red with its NZ atom highlighted in yellow, denoting its positive charge. Glutamic acid (^{II}Glu118), characterized by a negative charge, is colored in blue, with its OE1 and OE2 atoms marked in yellow. Panel B features histograms that display the distribution of distances between ^{II}Glu118 and ^{II}Lys159 prior to the disassociation of their interaction, with a specified cutoff at 12.5 ns. These histograms are based on data from six simulations, with three each under conditions of applied force and no-force. The black solid line indicates the Kernel Density Estimate (KDE) for the condition where force is applied, while the black dashed line represents the KDE for the no-force condition.

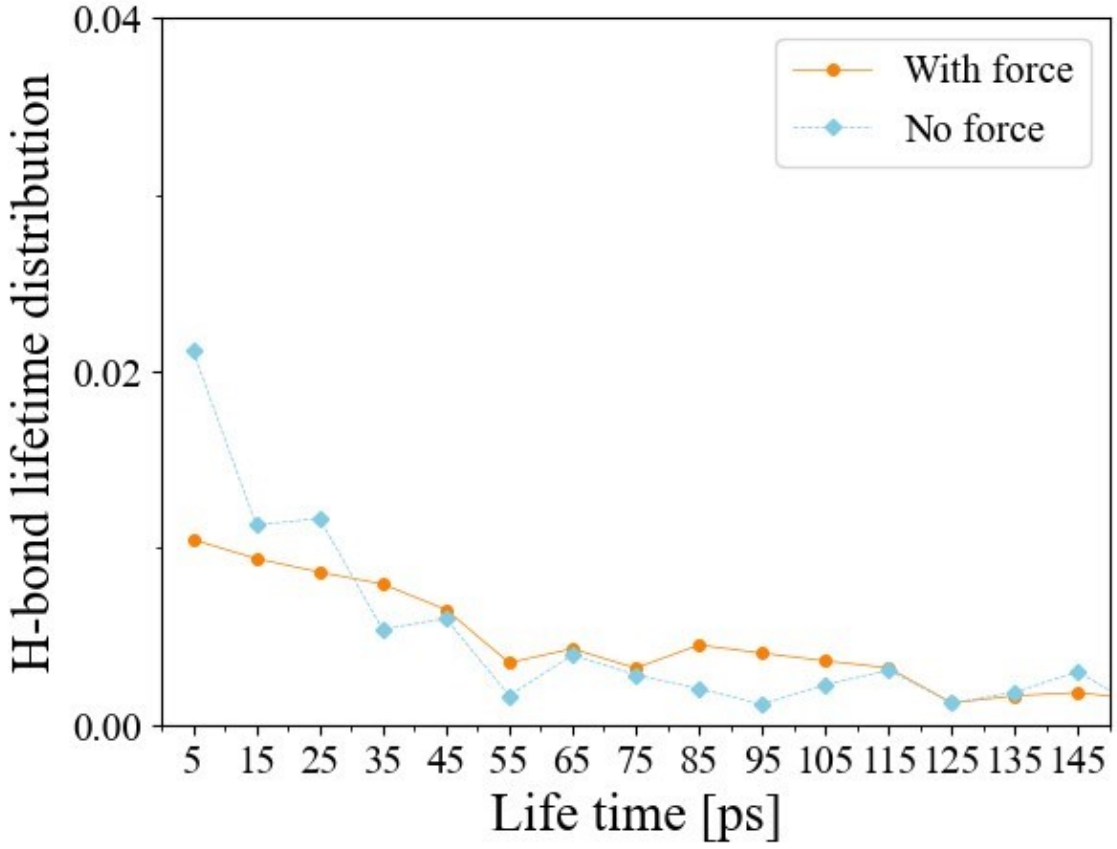

Supplementary Figure S4: Comparative Analysis of Hydrogen Bond (H-bond) Lifetimes for the ^{I}Asn157-^{II}Glu162 Interaction in Different Conditions. This figure presents the distribution of H-bond lifetimes for the specified interaction, both under force-applied and no-force scenarios, up to the predetermined breakage cutoff. Data is compiled from all six simulations, with three simulations (N=3) conducted for each condition (force and no-force). This comparison highlights the impact of applied force on the stability and duration of the ^{I}Asn157-^{II}Glu162 hydrogen bond.

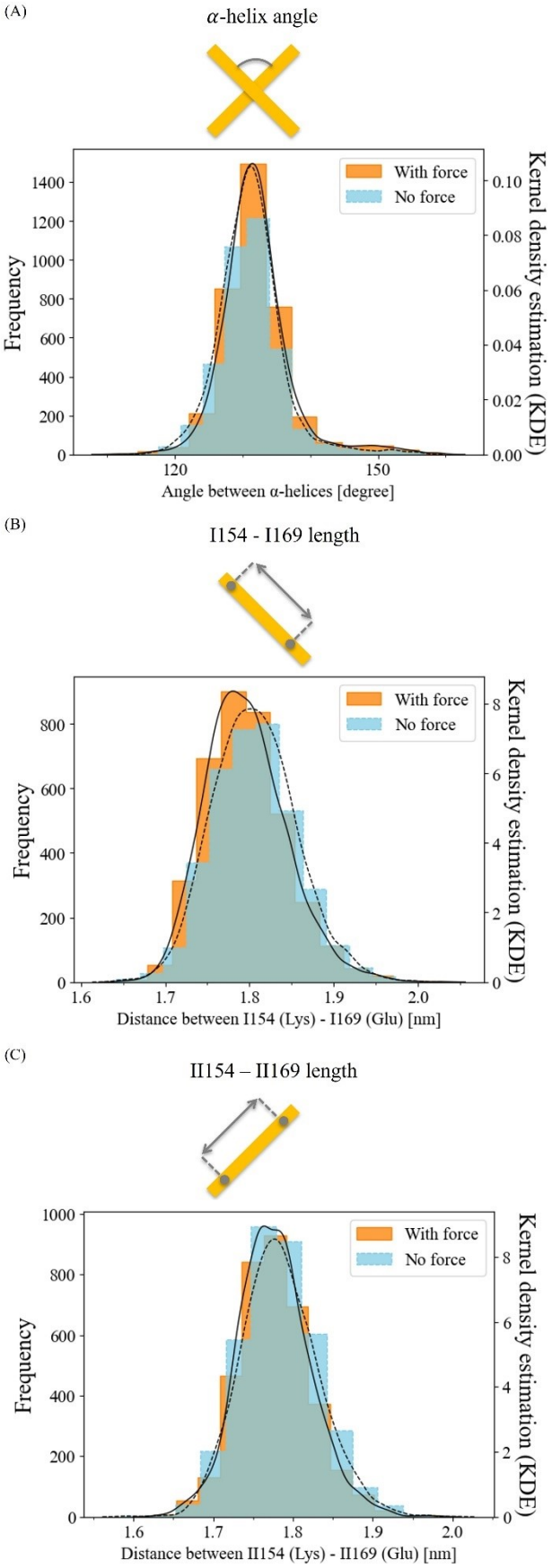
(A)
α-helix angle
With force
No force
Frequency
Kernel density estimation (KDE)
Angle between α-helices [degree]
(B)
I154 - I169 length
With force
No force
Frequency
Kernel density estimation (KDE)
Distance between I154 (Lys) - I169 (Glu) [nm]
(C)
II154 – II169 length
With force
No force
Frequency
Kernel density estimation (KDE)
Distance between II154 (Lys) - II169 (Glu) [nm]

Supplementary Figure S5: Comparative Analysis of Angle and Length Frequencies in the CSD-CSD Dimer. This figure features histograms that demonstrate (A) the frequency distribution of angles between the two α-helices of the CSD-CSD dimer, and the frequency distribution of the lengths of residues ^{I}Lys154-^{I}Glu169 (B) and ^{II}Lys154-^{II}Glu169 (C), up to the interaction breakage cutoff of 12.5 ns. These distributions are shown for both conditions with applied force and without force across all six simulations (N=3 for each force/no-force condition). The black solid lines in the histograms denote the Kernel Density Estimation (KDE) for the force-applied condition, whereas the black dashed lines indicated the KDE for the scenarios without force.

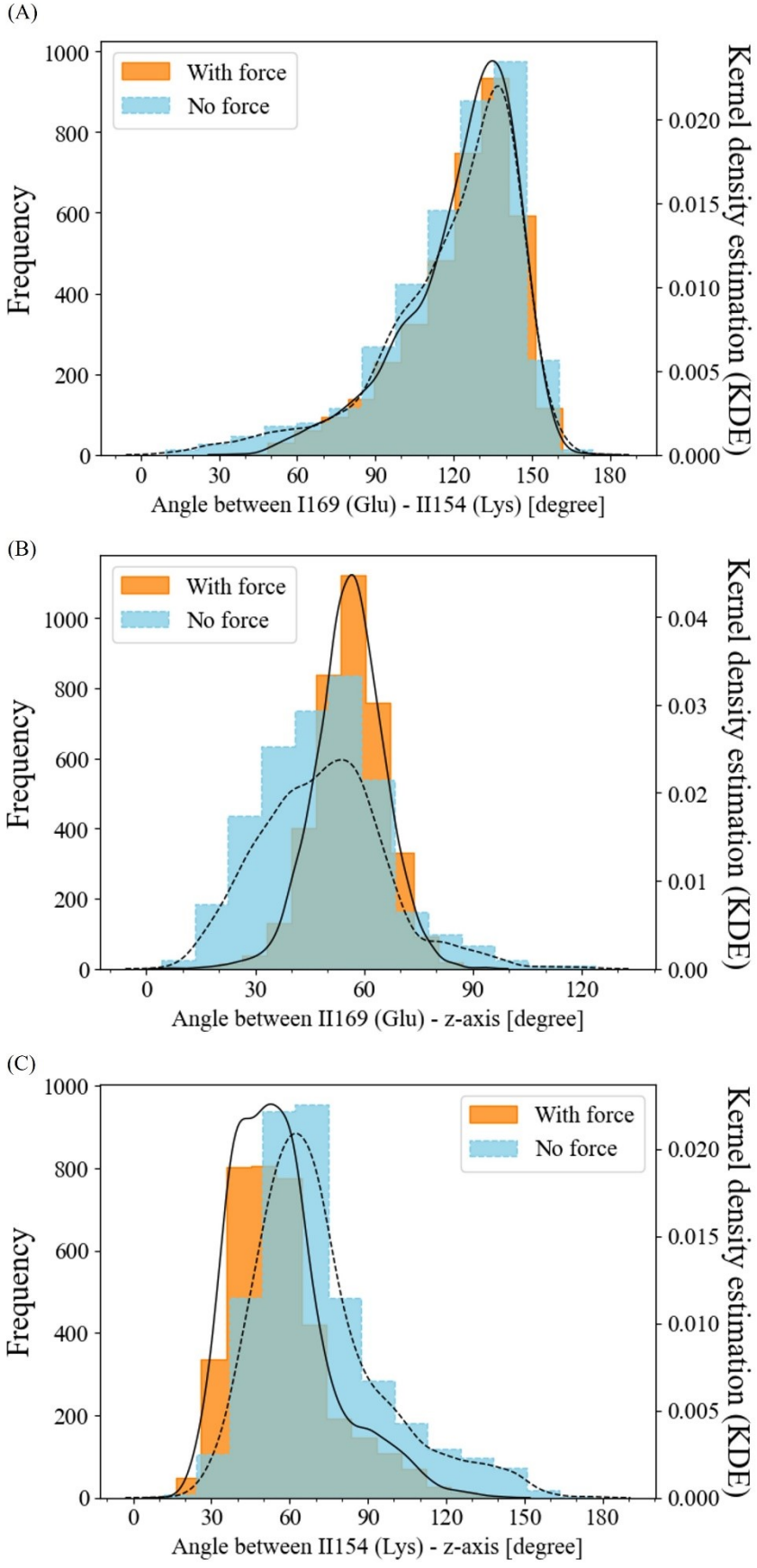
(A)
With force
No force
Frequency
Kernel density estimation (KDE)
Angle between I169 (Glu) - II154 (Lys) [degree]
(B)
With force
No force
Frequency
Kernel density estimation (KDE)
Angle between II169 (Glu) - z-axis [degree]
(C)
With force
No force
Frequency
Kernel density estimation (KDE)
Angle between II154 (Lys) - z-axis [degree]

Supplementary Figure S6: Analysis of Angle Frequency Distributions in the CSD-CSD Dimer Interactions. This figure presents histograms that illustrate the frequency of angles between (A) ^{I}Glu169 and ^{II}Lys154, (B) ^{I}Glu169 and the z-axis, and (C) ^{II}Lys154 and the z-axis, up to the predetermined interaction breakage cutoff of 12.5 ns. Data is shown for both scenarios: with applied force (force condition) and without applied force (no-force condition), across all six simulations (N=3 for each condition). In these histograms, the black solid lines denote the Kernel Density Estimation (KDE) for the force-applied condition and the black dashed lines represent the KDE for the no-force condition.

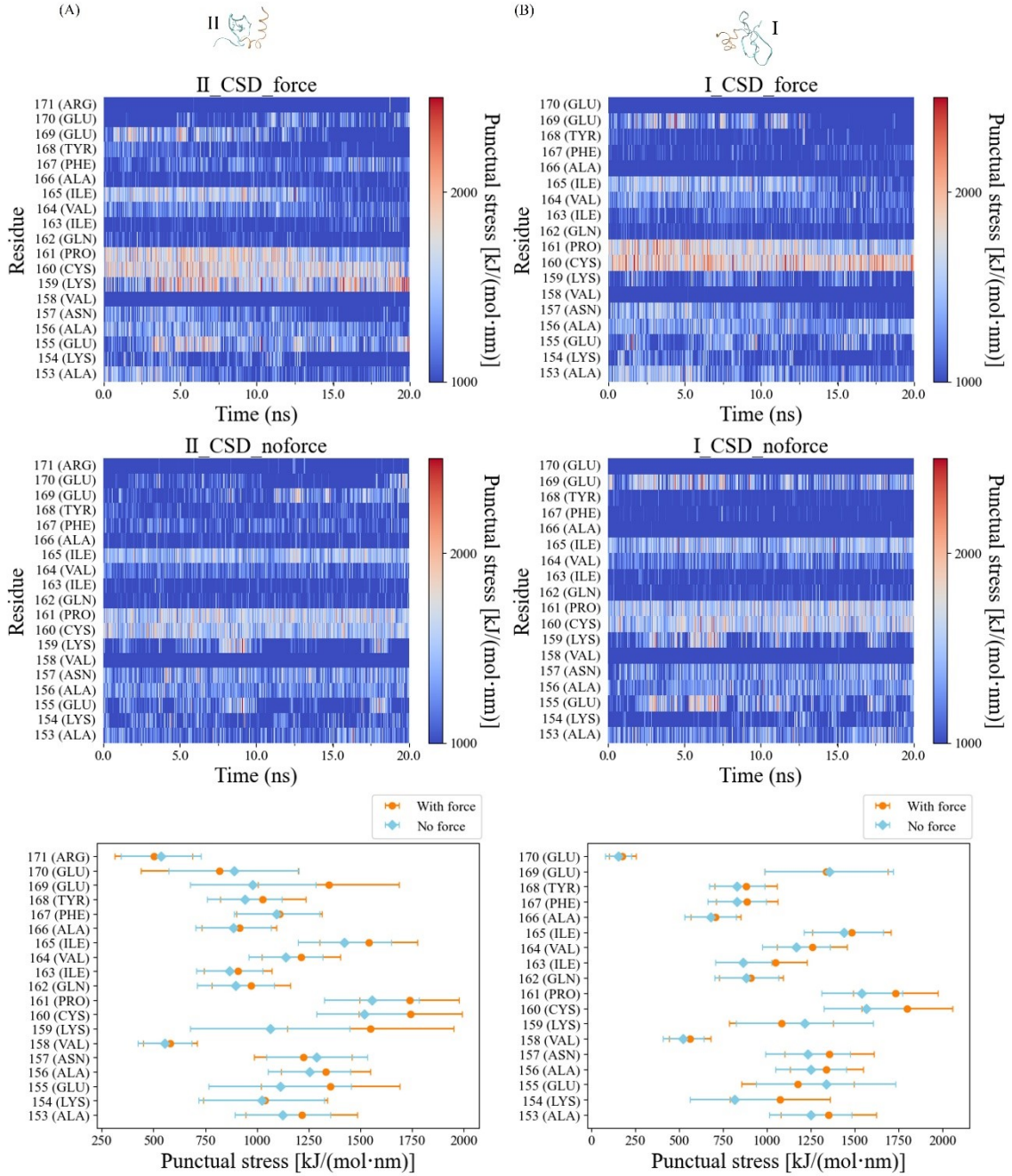

Supplementary Figure S7: Lennard-Jones Interaction-Based Force Distribution Analysis in ^{I}CSD Monomers. Panel (A) illustrates the force distribution in the Constrained ^{II}CSD monomer (left), and Panel (B) depicts the same for the Unconstrained ^{I}CSD monomer (right), along the α-helix interface. These analyses consider scenarios with and without applied force over a 20 ns simulation period. The heatmaps, reflecting Lennard-Jones-based punctual stress, were created

by averaging the data from three simulations at each time step, under both force-applied and no-force conditions. Accompanying bar plots quantify the average punctual stress across residues, including standard deviations, based on data collected prior to the bond breakage cutoff at 12.5 ns.

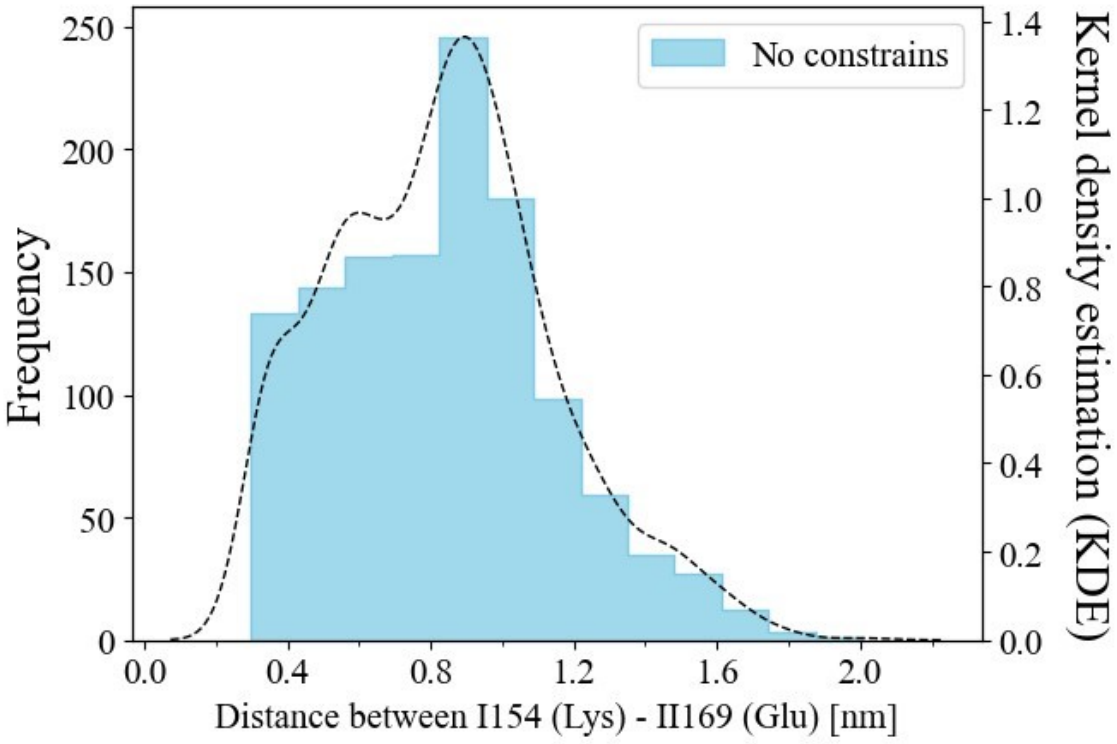

Supplementary Figure S8: Distance Frequency Analysis for ILys154-IIGlu169 Interaction. This figure presents histograms depicting the frequency distribution of distances between ^{I}Lys154 and ^{II}Glu169 residues over a 20 ns simulation period, conducted without any positional constraints.

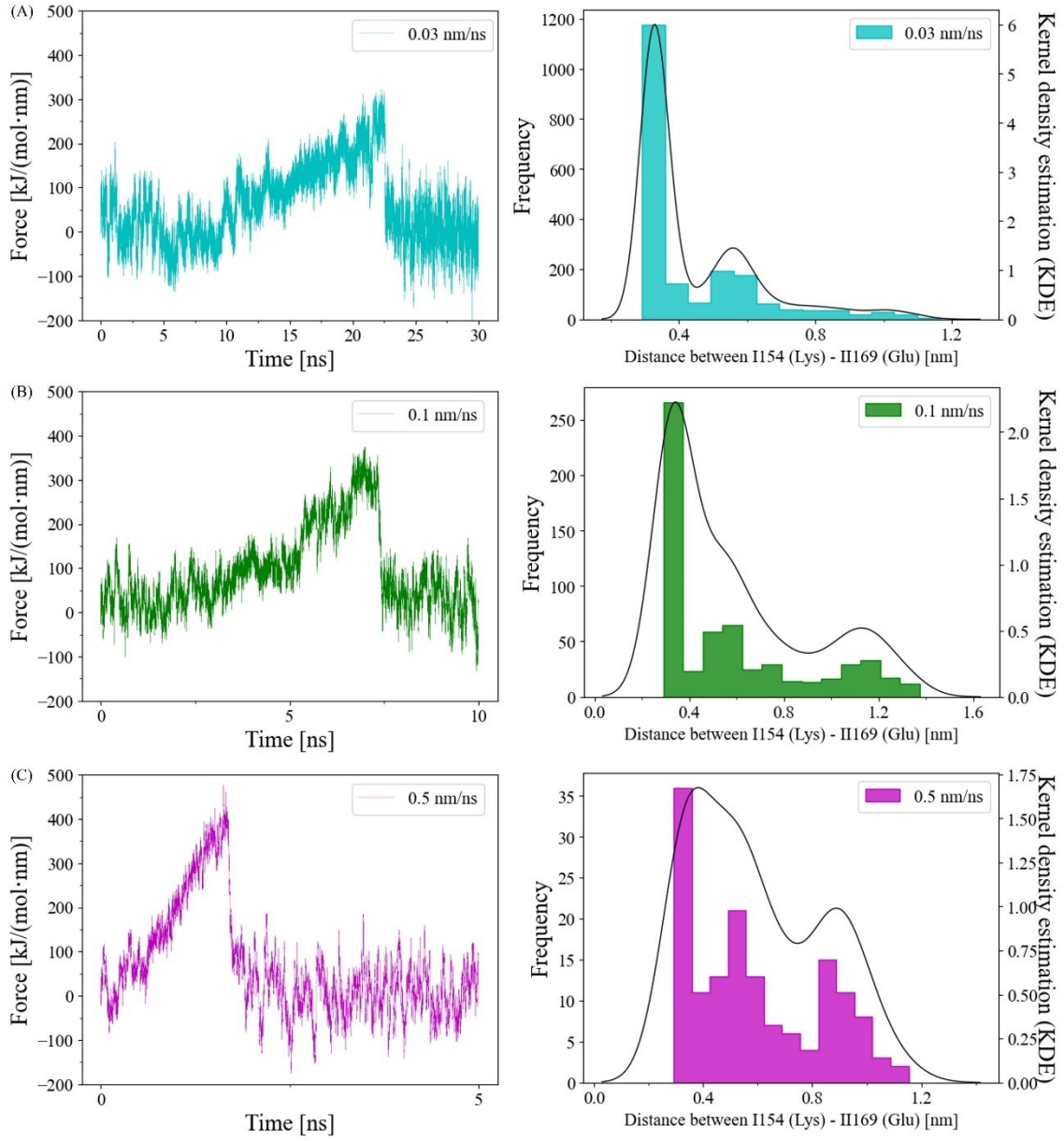

Supplementary Figure 9: Analysis of Harmonic Pulling Forces and Salt Bridge Pair Distances. The left panel displays the application of pulling harmonic forces at pull rates of (A) 0.03, (B) 0.1, and (C) 0.5 nm·ns^{-1}. Accompanying histograms depict the frequency of distances between the ^{I}Lys154-^{II}Glu169 salt bridge pair prior to interaction breakage. Based on the force profiles, cutoff times for analysis at the respective pull rates of (A) 0.03, (B) 0.1, and (C) 0.5 nm·ns^{-1} have been determined to be 20, 6, and 1.5 ns, respectively.